Solid Freeform Fabrication 2024: Proceedings of the 35th Annual International Solid Freeform Fabrication Symposium – An Additive Manufacturing Conference
Reviewed Paper

Compressive strength of 3D printed 17-4 PH honeycomb structure

Haijun Gong[1], Juan Sierra[1], Reece Woodard[1], Yue Zhang[1], Lianjun Wu[1], Shaowen Xu[2]

[1]Department of Manufacturing Engineering, Georgia Southern University, Statesboro, GA 30460
[2]Department of Mechanical Engineering, Georgia Southern University, Statesboro, GA 30460

Abstract

Engineered honeycomb structures are commonly used to reduce part weight and material usage. However, the traditional manufacturing processes for honeycomb structures are inflexible and only limited to simple shapes. With 3D printing, the honeycomb structure can be effectively manufactured and integrated into complex part designs. This study adopted the newly introduced metal-polymer filament of 17-4 PH stainless steel and conducted fundamental research about the compressive strength and engineering-absorption capability of 17-4 PH honeycomb structures fabricated sequentially by material extrusion based 3D printing, debinding, and sintering. Compression testing was performed to evaluate the in-plane compressive strength of the honeycomb structure. The stress-strain curve was acquired to identify the plastic collapse and densification onset, to further understand its energy-absorption capability. Microscopic observation and fractography were also conducted to discuss the failure mode under the compression loading scenario.

Introduction

Material extrusion (MEX) based 3D printing process for metal parts is of great interest to researchers and engineers in recent years due to its low-cost equipment investment and uncomplicated operations [1]. Commercialized metal-polymer filaments and 3D printing equipment have been introduced to the market for making MEX metal parts. Especially, the BASF *Ultrafuse* 316L and 17-4 PH metal filaments are attracting many end users to print green parts using MEX printers and outsource debinding/sintering services to achieve metal 3D printing parts. Studies on optimizing filament usage parameters and characterizing MEX metal properties are receiving more attention in the additive manufacturing community.

Gong et al. compared the hardness, tensile strength, and microstructures of stainless steel 316L printed by MEX and SLM process [2]. The anisotropic shrinkage of MEX 316L part was pointed out in their study. Pellegrini et al. further studied the shrinkage anisotropy of 17-4 PH parts in terms of the printing parameters [3]. The fatigue life of MEX 316L component and its failure mechanisms were investigated, showing a lower fatigue limit compared to wrought 316L [4]. The porosity was reported to be an issue of lowering the part strength [5]. Fazzini et al. studied the effects of extrusion parameters and filling pattern of 17-4 PH filament on the metal part's mechanical properties [6]. The study identified the critical parameter influencing the tensile strength. Lots of research is ongoing and implies a growing interest in this 3D printing process. However, the studies on MEX printing metal lightweight structures, such as lattice or honeycomb, are limited. Jiang et al. fabricated unit lattice structures using 17-4 PH filaments and evaluated the physical deformation and compressive properties through modeling, simulation, and experiment [7]. The testing focused on three plate-lattice structures. Obadimu et al. studied the compressive

mechanical properties of honeycomb structure printed using *Ultrafuse* 316L filament. It was found that the deformation mechanism/mode is cell size and load-rate dependent [8]. There are few studies on the MEX honeycomb structures of 17-4 PH material. To enrich the research in MEX lightweight structures of metal, this project concentrates on the compressive strength (in-plane) and energy absorption capability of 17-4 PH honeycomb structures. Porosity and honeycomb fracture are also analyzed in this study.

Experiment

The honeycomb structure was designed with regular geometry using *Solidworks*, as shown in Fig. 1. The overall size, as well as edge length and wall thickness, is determined based on the force capacity of the testing machine with an estimation of the breaking load not too high or too low. The CAD file was converted to STL and printed using a Flashforge Creator Pro 3D printer, with the feedstock of BASF *Ultrafuse* 17-4 PH filament. The debinding and sintering processes were outsourced to make the green parts to be pure metal parts. Fig. 1(c) shows an apparent shrinkage of the metal honeycomb structure. Keyence *VR-3000* macroscope was employed to measure the honeycomb edge length and wall thickness to estimate its actual relative density. To evaluate the compressive strength (in-plane) of 17-4 PH honeycomb, an ADMET *MTESTQuattro* universal tester was used to conduct the compression test via the same testing procedure. In addition, the solid 17-4 PH density was measured using a Micromeritics *AccuPyc II 1340* gas pycnometer. An Olympus BX53 optical microscope was used to observe the defect distribution on the sectioned/polished hexagonal unit cell. The fractography was imaged using a Phenom™ XL G2 Desktop SEM.

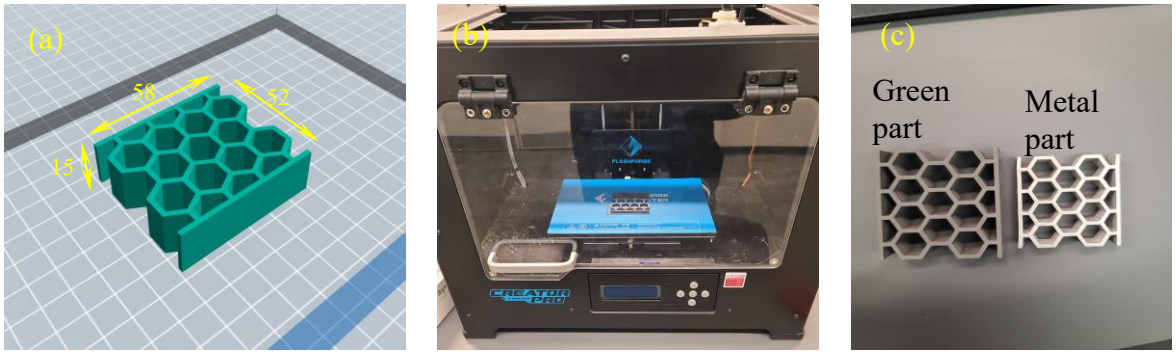

Fig. 1 Honeycomb structure design and 3D printing for metal part (unit: mm)

Results and Discussion

Density and porosity

Small 3D printed 17-4 PH pieces were inserted into the pycnometer cup to measure the actual density of the solid material. The value of 7.55 g/cm^3 indicates an approximate porosity of 3.2%, as compared to the nominal density of 17-4 PH stainless steel (7.80 g/cm^3). With the consideration of MEX 3D printing's infilling pattern, the inherent void inclusion is unavoidable. Hence, a small percentage of porosity in the printed honeycomb structure is normal. To further understand the defect distribution is more beneficial to analyze the honeycomb structure's mechanical performance and fracture behavior. The hexagonal unit cell of 17-4 PH was mounted and polished to study the defect inclusion. As shown in Fig. 2, the defect distribution presents a significant unevenness all over the sectioned area. Defects exhibit a continuity along the edge direction of the honeycomb structure. Most areas only include a small number of defects, while some local areas

present a serious accumulation of defects. The unevenness might be attributable to the infilling strategy of the MEX 3D printing process. The cross-section area and honeycomb wall thickness are all believed to influence the infilling of extruded material to each layer. To better predict the defect distribution, the scan strategy for the honeycomb or lightweight structure (small cross-section area) deserves further investigation.

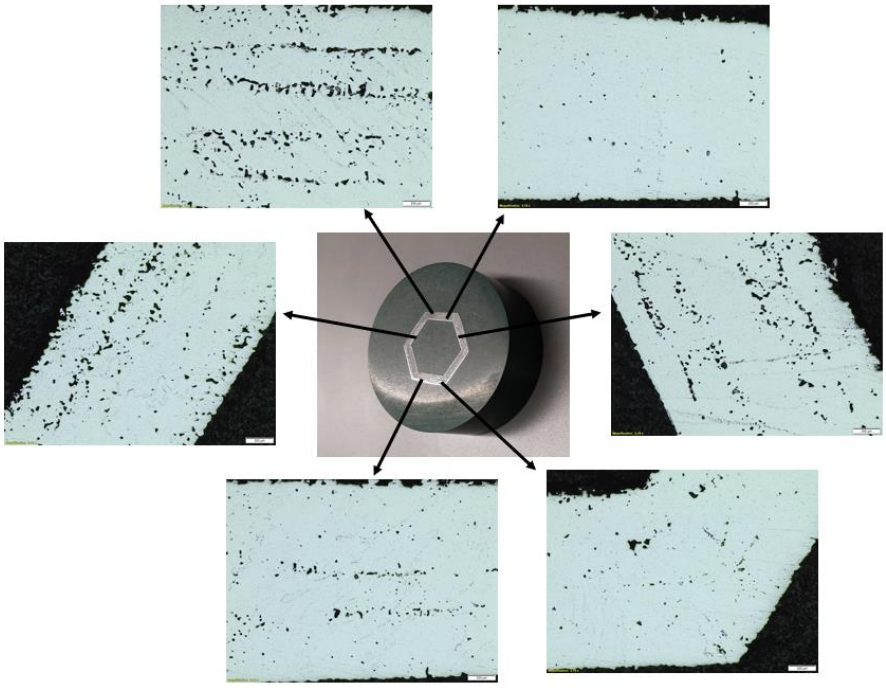

Fig. 2 Microscopy of 17-4 PH honeycomb unit cell

Shrinkage and size variation

The actual size of the green part is very close to the nominal size of the CAD file (58×15×52 mm, as shown in Fig. 1(a)). After debinding and sintering process, the overall size of the metal honeycomb is decreased to ~48×11.5×44 mm. A *Keyence* macroscope was used to measure the actual wall thickness and edge length of the metal honeycomb unit cell (Fig. 3). The relative density of the honeycomb structure is found to be close to the CAD file of the designed honeycomb based on Equation (1), even though an apparent shrinkage can be observed after sintering. The calculated density of the metal honeycomb structure is around 2.18 g/cm^3.

$$\frac{\rho^*}{\rho_s} = \frac{2}{\sqrt{3}}\frac{t}{l} \qquad (1)$$

Where,
ρ^* is the density of the honeycomb
ρ_s is the density of solid 17-4 PH
t is the wall thickness
l is the edge length

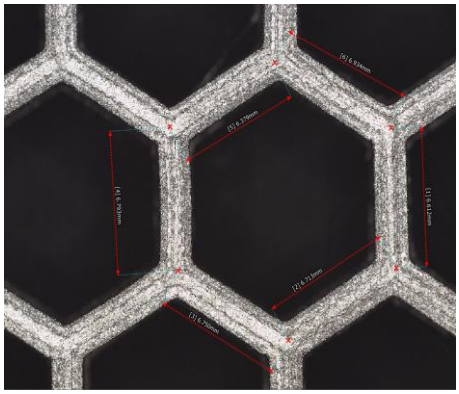

Fig. 3 Metal honeycomb structure for measurement

Compressive strength

5 samples underwent compression testing to determine the compressive strength of the 17-4 PH stainless steel honeycomb structure. Stress-strain curves (Fig. 4) were plotted from the calculated data to feature the energy absorption capability of the honeycomb structures.

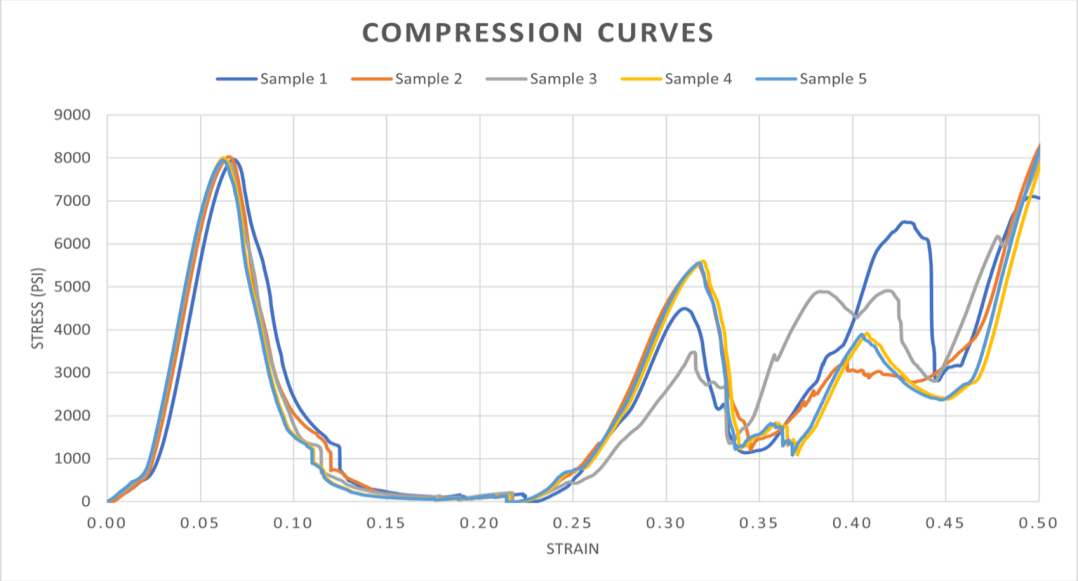

Fig. 4 Stress-stain curves of 17-4 PH honeycomb structures

It is noted that at the very beginning of the compression, the curve has a short distortion before the elastic deformation. This is attributed to the inferior parallelism of the two flat plates of the specimen. After the debinding and sintering process, the green part's geometrical accuracy is more or less influenced, resulting in a decreased flatness of the plates. The tester's crossheads touch the specimen during compression and cause a slight specimen distortion. After the honeycomb was completely secured between the crossheads, the honeycomb was elastically deformed with stress up to around 8000 psi, as shown in Fig. 4. The hexagonal unit cells were then subjected to brittle fracture at the proximity of nodes of the honeycomb immediately when the stress dropped down. It is interesting to see that the fractures took place along a ~45° angle between two plates (Fig. 5), indicating a nearly isotropic mechanical property of the honeycomb structure. When the honeycomb is completely fractured, stress is down to zero, as shown in the stress-strain curve. However, the honeycomb structure is still capable of absorbing energy through the plastic collapse. The broken pieces interact with each other to densify the honeycomb. The fluctuation of the stress-strain curve illustrates the continuous energy absorption during the compression process.

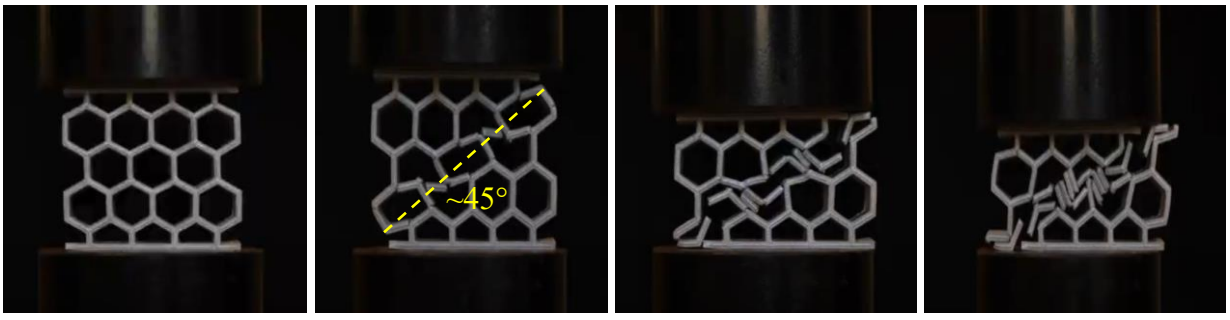

Fig. 5 Compression of 17-4 PH honeycomb structure

Fractography

The fracture surface was observed using SEM. It can be seen from the SEM image that the failure of the honeycomb structure is composed of both brittle and ductile fractures during the compression process. The inherent voids (Fig. 6) of 3D printed 17-4 PH play a critical role in the crack initiation and propagation of the structure fracture. The cracks propagate towards the sharp edge of the voids where the maximum stress concentration is located. The brittle fracture surface is formed through the crack propagation. When multiple small cracks accumulate to a certain extent, the cross-section of the honeycomb structure edge fails to sustain the load and causes a sudden rupture. The ductile features of the disruptive fracture are exhibited with dimples and coarse surfaces across the fracture surface.

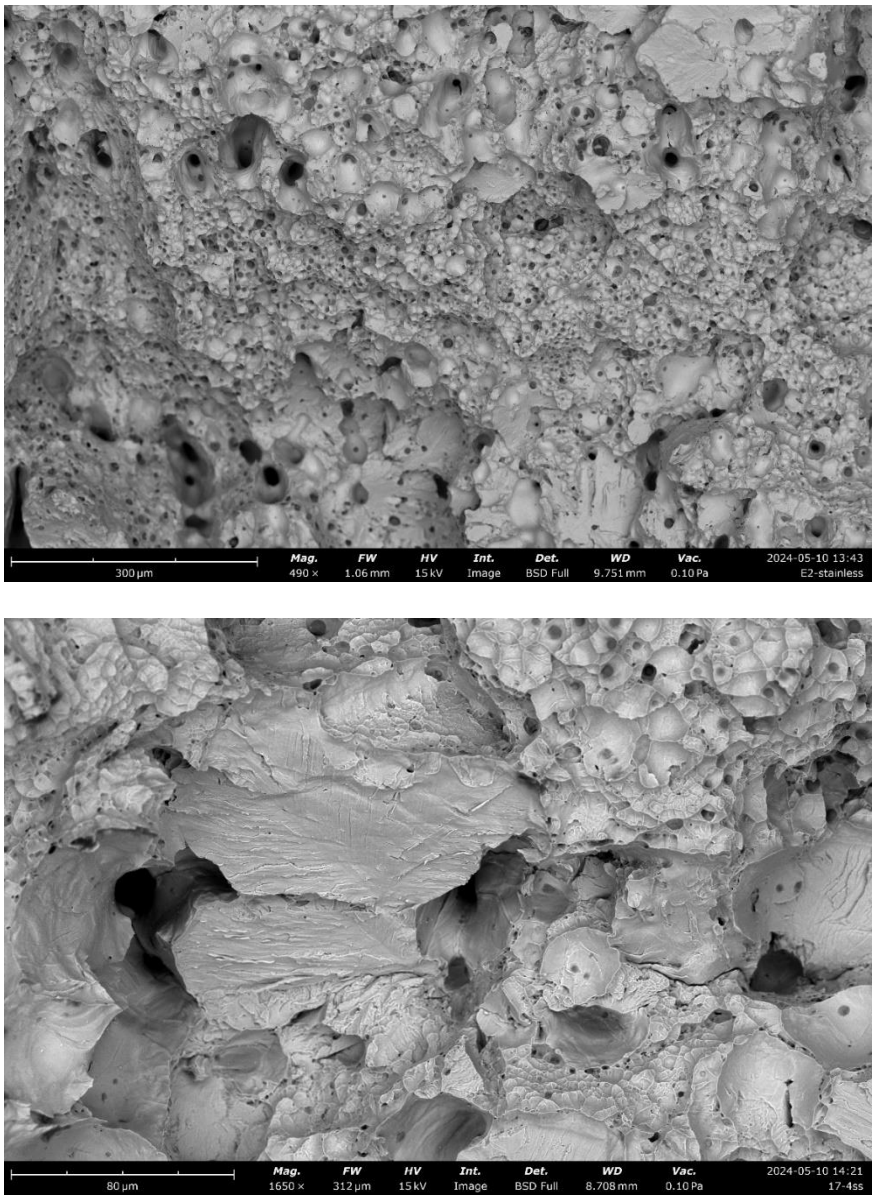

Fig. 6 The fracture surface of 17-4 PH honeycomb structure

Conclusion

The MEX 3D printing process can make honeycomb structures using *Ultrafuse* 17-4 PH filament. The compression test result is strong evidence that the printed metal honeycomb can resist certain compression loads and continuously absorb energy, even though the inherent voids are unevenly distributed in the material. A nearly isotropic mechanical property can be predicted based on the inclined failure plane (~45°) of the honeycomb structure. The included defects are the primary crack initiation sites, followed by crack propagation and edge fractures of the hexagonal unit under the compression loads. Defect mitigation and shrinkage compensation deserve further studies for MEX 3D printing honeycomb structures.

Reference

[1] Y. Thompson, J. Gonzalez-Gutierrez, C. Kukla, P. Felfer (2019). Fused filament fabrication, debinding and sintering as a low cost additive manufacturing method of 316L stainless steel, Additive Manufacturing, 30, 100861.

[2] H. Gong, D. Snelling, K. Kardel, A. Carrano (2019). Comparison of stainless steel 316L parts made by FDM-and SLM-based additive manufacturing processes, JOM, 71(3), 880-885.

[3] A. Pellegrini, M. G. Guerra, F. Lavecchia (2024). Shrinkage evaluation and geometric accuracy assessment on 17-4 PH samples made by material extrusion additive manufacturing. Journal of Manufacturing Processes, 109, 394-406.

[4] S. Spiller, S. O. Kolstad, N. Razavi (2023). Fatigue behavior of 316L stainless steel fabricated via Material Extrusion Additive Manufacturing, Engineering Fracture Mechanics, 291, 109544.

[5] S. Spiller, S. O. Kolstad, N. Razavi (2022). Fabrication and characterization of 316L stainless steel components printed with material extrusion additive manufacturing, Procedia Structural Integrity, 42, 1239-1248.

[6] F. Fazzini, A. Boschetto, L. Bottini, A. C. Diez, A. Cini (2023). Correlation between metal fused filament fabrication parameters and material properties of sintered 17-4 PH, Procedia Structural Integrity, 49, 59-66.

[7] D. Jiang, F. Ning (2023). Physical-mechanical behaviors of stainless steel plate-lattice built by material extrusion additive manufacturing, Procedia Structural Integrity, 49, 59-66.

[8] S. O. Obadimu, K. I. Kourousis (2022). Load-rate effects on the in-plane compressive behaviour of additively manufactured steel 316L honeycomb structures, Engineering Structures, 273, 115063.